

STRUCTURAL ANALYSIS OF SEPIOLITE BY SELECTED AREA ELECTRON DIFFRACTION—RELATIONS WITH PHYSICO-CHEMICAL PROPERTIES

M. RAUTUREAU* and C. TCHOUBAR

Laboratoire de Cristallographie, Université d'Orléans, et Centre de Recherche sur les Solides à Organisation Cristalline Imparfaite C.N.R.S., Orléans, France

(Received 22 May 1975)

Abstract—The electron structural analysis of a Madagascar sepiolite (Ampandrandava) was carried out by selected area electron diffraction obtained from monocrystals. Fourier projections, derived from the experimental intensity of Ok_l , $h0l$ and $hk0$ reflections, show that the Mg^{2+} cations on the edges of the sheets are distributed between two sites. Correlatively the water molecules bound to these Mg^{2+} occupy two distinct positions. These principal structural differences with the Brauner and Preisinger model explain details of the i.r. spectra during the desorption of water or the adsorption of polar molecules. The differences between the two models can be considered as a consequence of treating the mineral in vacuum.

INTRODUCTION

Sepiolites belong to a magnesian group of silicates, with a fibrous texture, whose ideal formula can be written $Si_{12}Mg_8O_{32} \cdot nH_2O$. Structural analyses were made first by Nagy and Bradley (1955), then by Brauner and Preisinger (1956) from X-ray powder diffraction data. They showed that this mineral can be schematized by a quincunx† arrangement of talc type layers separated by parallel channels with dimensions *ca.* $7 \times 13 \text{ \AA}$ (Fig. 1).

This microporosity gives sepiolites a unique place in the clay family because of its structural character-

istics and physico-chemical properties. Nevertheless, the relations between certain properties of sepiolite and its structure are still poorly understood. Previously this mineral, which is both microcrystalline and fibrous, has been studied only with powder or fibrous aggregate diagrams. Under these conditions it is not possible to make a precise structural analysis. In particular, the structural model proposed by Brauner and Preisinger, although confirmed in its general form by various authors (Brindley, 1959; Zvyagin, 1967; Martin-Vivaldi and Robertson, 1971; Rautureau *et al.*, 1972), is too idealized to allow a better interpretation of the phenomena connected with the existence of water molecules in the channels and the internal surface of sepiolite (water desorption or polar molecule fixation, for instance).

The present work uses structural analysis of a well-crystallized sepiolite (Ampandrandava sepiolite, Madagascar) by selected area electron diffraction

* This work is a part of the Doctoral Thesis of M. Michel Rautureau, 1974, University of Orleans, France.

† Quincunx "A disposition of five objects so placed that four occupy the corners and the fifth the center of a square or rectangle" (*Oxford Universal Dictionary*, 3rd Edn., revised 1955, p. 1642).

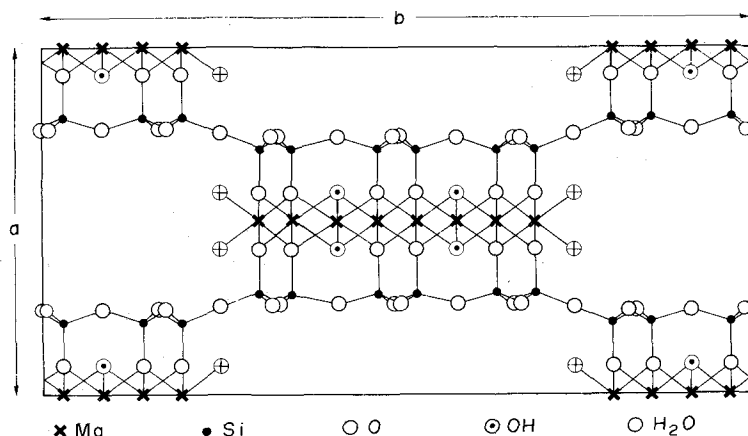


Fig. 1. Schematic (001) projection of atoms of sepiolite unit cell showing the quincunx arrangement of talc type layer.

which is the only technique for obtaining monocrystal patterns for a very finely divided mineral. A Philips model EM 300 electron microscope equipped with an anticontamination device and with a tilt stage specimen holder was used for this work. The integrated intensity of each reflection was measured by means of a flying spot microdensitometer (Joyce Loebel model) on the electron diffraction pictures.

PREPARATION OF SAMPLES AND CHOICE OF MONOCRYSTALLIZED PARTICLES FOR STRUCTURAL STUDIES

Using natural aggregates of sepiolite fibers, two types of samples were prepared:

(a) The aggregates were dispersed in a water suspension and a drop of the suspension was deposited on a carbon membrane. In a sample of this type, the electron beam crosses the fibers perpendicular to their axis. With these samples reflections Ok_l or reflections hOl occur in the same pattern (sepiolite is of orthorhombic symmetry and the c -axis was chosen parallel to the fiber axis).

(b) Fiber aggregates were embedded in a polymer and cut with a diamond knife perpendicular to the fiber axis (Tchoubar *et al.*, 1973). The electron beam is then parallel to the fiber axis and hkO reflections are obtained.

In order to determine the possibility of employing Fourier synthesis on the basis of a kinematic model, a preliminary morphological study was carried out to choose suitable monocrystals (Rautureau and Tchoubar, 1972). The particles of sepiolite are similar to elongated laths whose thickness varies between 150 and 1000 Å (see Fig. 2). The thickness is controlled by means of a Pt-C shadowing in this case.

Similarly, the transverse sections of sepiolite were studied with the "lattice imaging"* technique (the thickness of the sections was approx. 500–600 Å). This method permits observations of the interference image of some diffracted beams. Figure 3(a and b) show two examples of sepiolite particles cut perpendicularly to the c -axis. These pictures were obtained from interferences between the 000 , 020 and 110 . Figure 3(a) shows a monocrystal in which are distinguished two systems of undeformed parallel fringes, equidistant at ca. 12 Å and with an angle of 60°. This double system of well-defined fringes correspond with the $\overset{\pm}{1}\overset{\pm}{1}0$ reflections whose intensity is approx. 25 times greater than that of the $0\overset{\pm}{2}0$ reflections. Figure 3(b) gives an example of the section of a large sepiolite crystal. The existence of numerous faces $\{110\}$ and a great tubular porosity whose cross section is between 20 and 200 Å can be seen. In much of this double system corresponding to the $\overset{\pm}{1}\overset{\pm}{1}0$ reflections, fringes equidistant at 27 Å with a variable definition can be observed. The last system of fringes suggests the existence of dyna-

mic interactions due to the very important thickness of the section. Finally, Fig. 3(c and d) show an image of a monocrystal of sepiolite obtained by the interferences of the 000 beam with the $0\overset{\pm}{2}0$, $\overset{\pm}{1}\overset{\pm}{1}0$, $\overset{\pm}{2}00$ and $\overset{\pm}{1}\overset{\pm}{1}30$ beams (Fig. 3c is a general view and the magnified region is shown in Fig. 3d). The quincunx arrangement of the elements of layers, in agreement with the structural scheme of Brauner and Preisinger, can be seen in the last figure (5 elements of layers are schematized with a line). In crystal B at the top of Fig. 3(c) the fringes are well-defined in only one direction because the crystals are cut obliquely with respect to the c -axis. Crystal A is cut perpendicular to this axis.

The morphological results justify the application of the kinematic theory of diffraction. Theoretical studies by Cowley and Moodie (1962) and by Cowley (1968) show that the diffraction can be treated by kinematic theory for electrons accelerating under 100 kV when the thickness of the sample is not greater than a few hundred Angströms and the atomic number of the constituents is lower than 15. The morphological results show clearly that the tubular porosity reduces to some hundred Angströms the dimensions of the coherent crystalline domain crossed by the electrons perpendicular to the c -axis. Consequently, when the electron beam is perpendicular to the fiber axis, it is possible to use the reflections Ok_l and hOl independent of crystal thickness. On the other hand, in the hkO patterns, the intensities may be perturbed by the dynamic interactions because the thickness of the section is at least 500 Å.

STRUCTURE ANALYSIS OF SEPIOLITE BY MEANS OF ELECTRON SELECTED AREA MICRODIFFRACTION

Under the conditions in the electron microscope, with a vacuum of between 10^{-4} and 10^{-5} Torr, zeolitic water is eliminated from sepiolite and only the structural water bound to the edge of the layers is present (designated as H_2O_{cryst}). Thermogravimetric analysis and i.r. absorption spectra agree perfectly on this point (see Section IV). Preisinger (1963) showed the folding of the structure for sepiolite heated above 600°C. In his experimental conditions the sample is dehydrated. In the present work only the stage before dehydration is considered.

The microdiffraction data of the sample obtained from suspension agree with the extinction conditions of the space group $Pncn$. These are:

Ok_l with $k + l = 2n$ (Fig. 4a)

hOl with $l = 2n$ (Fig. 4b)

hkl without conditions, but with $h + l = 2n$ for $l = 0$ (Fig. 4c shows the reflections hkl)

The hkO reflections obtained in a section perpendicular to the c -axis (Fig. 4d) cannot be used because

* A general review of the applicability of "lattice imaging" is given by Allpress and Sanders (1973).

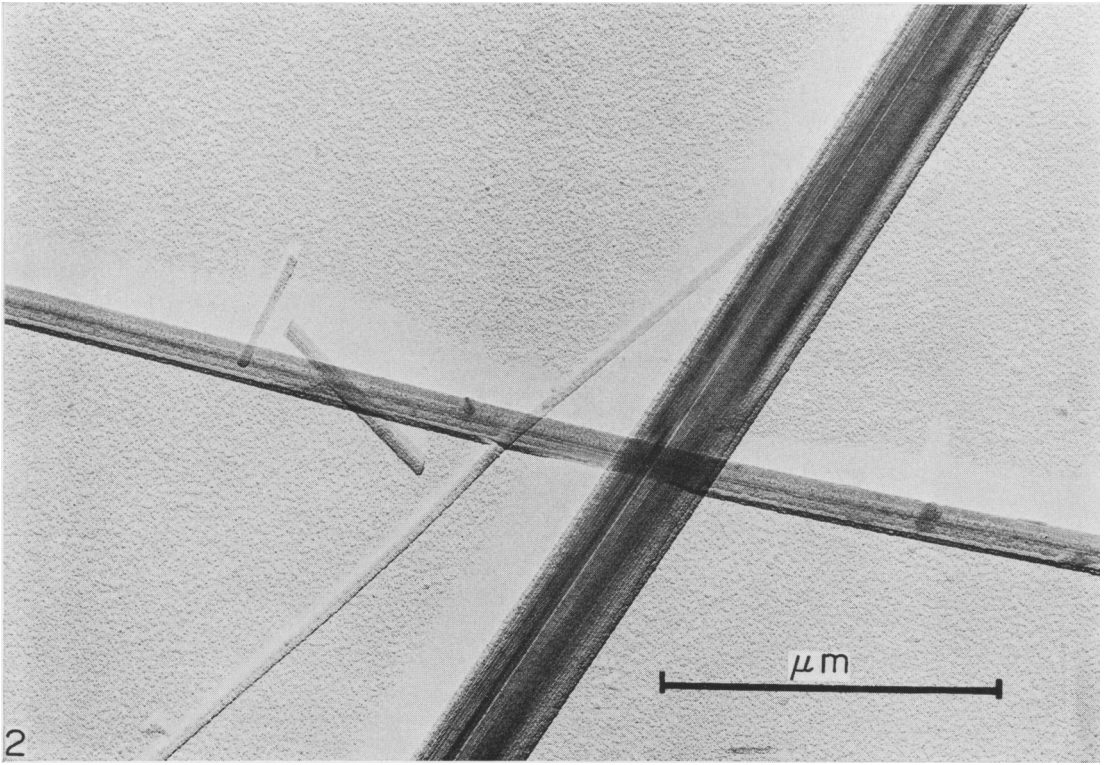


Fig. 2. Electron micrograph of Ampandrandava sepiolite fibers.

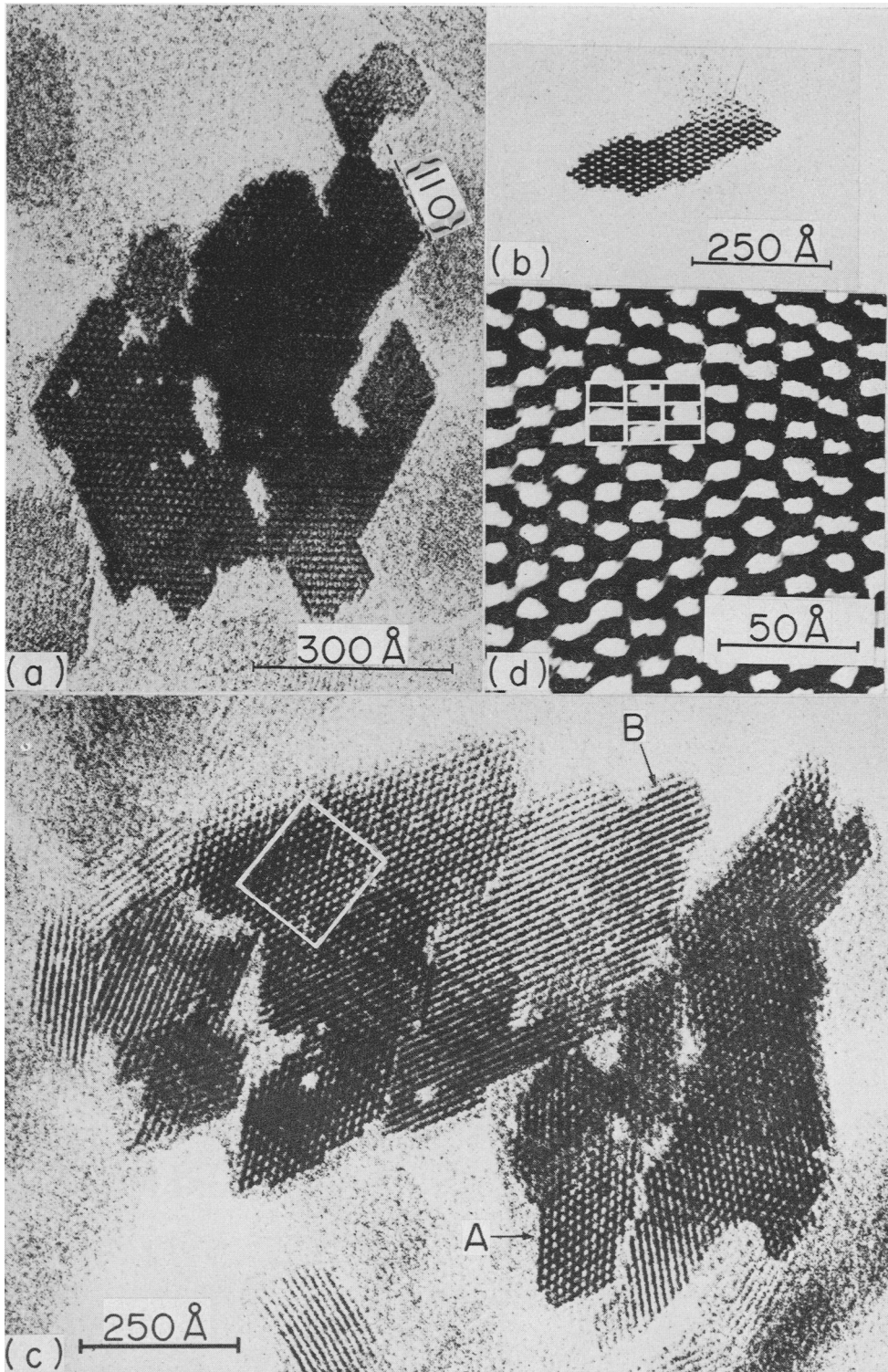


Fig. 3(a). Elementary fiber (monocrystal) of Ampandrandava sepiolite. (cut perpendicularly to the fiber axis). (b) Cross section of a monocystal of sepiolite showing numerous (110) faces and a great internal porosity. (c). Cross section of sepiolite of Ampandrandava (General view). (d) Magnified zone of the Fig. 5 with a direct view of channels.

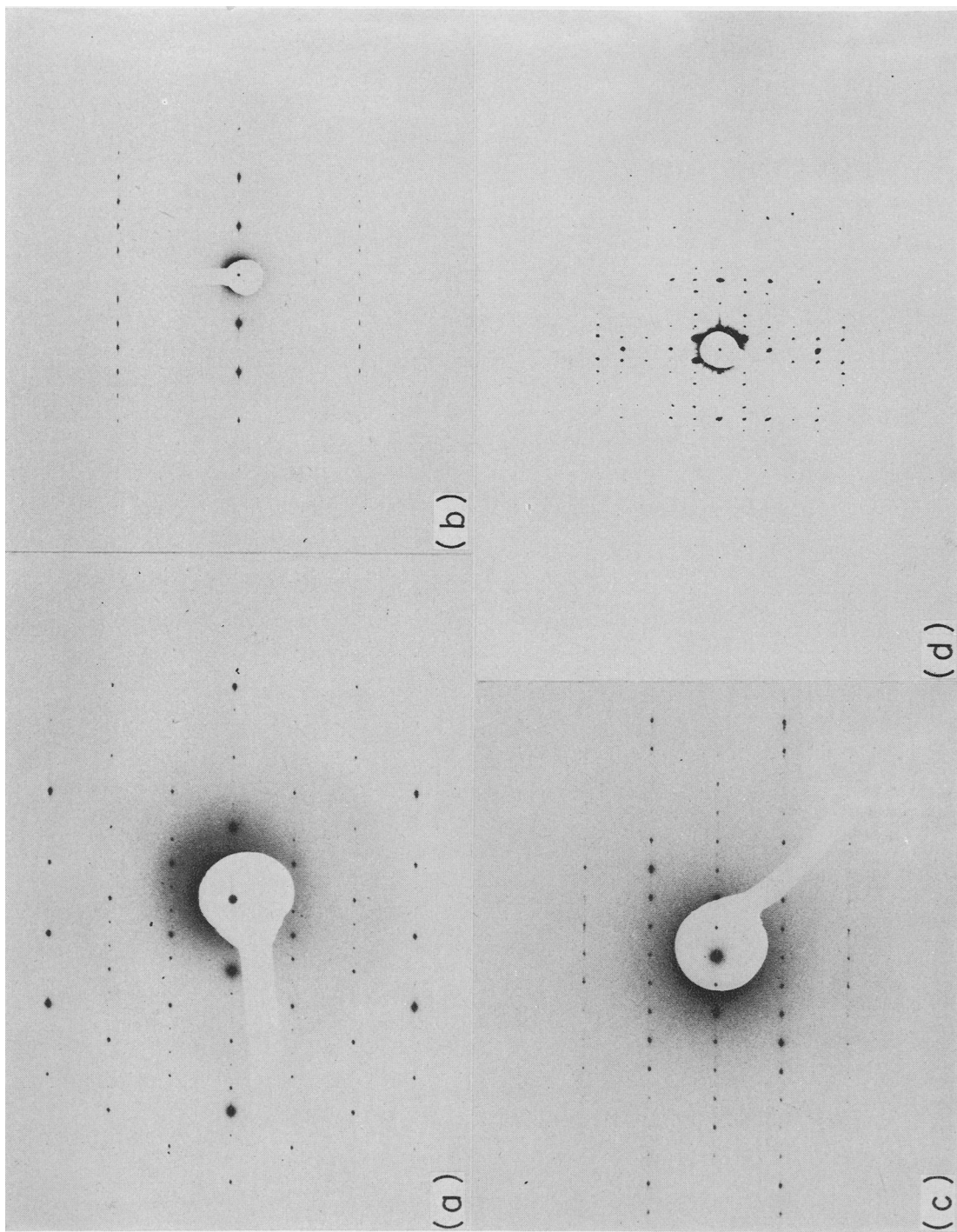


Fig. 4(a). Selected area diffraction of sepiolite: reflections Ok_l . (b). Selected area diffraction: reflection hOl . (c). Selected area diffraction: reflections hkl . (d). Selected area diffraction: reflections hkO .

the sections are much too thick. This is the cause of multiple diffraction.

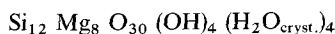
Parameter measurements on samples with a gold standard give the following values (Rautureau *et al.*, 1972):

$$\begin{aligned}
 a &= 13.37 \pm 0.04 \text{ \AA} \\
 b &= 26.95 \pm 0.08 \text{ \AA} \\
 c &= 5.27 \pm 0.02 \text{ \AA}.
 \end{aligned}$$

FOURIER PROJECTIONS

By using the measured intensities, $I_{obs.}$, of OkI reflections (68 reflections) and hOl reflections (31 reflections) a Fourier projection of the planes (100) and (010) for all atoms in the unit cell has been made.

For each model, the observed $|F_{hkl}|_{obs.} = |I_{hkl}|_{obs.}$, were normalized on the ten greatest calculated $|F_{hkl}|_{calc.}^2$. In all cases $|F_{000}|$ is the calculated value. The model initially utilized was that of Brauner and Preisinger (1956). Figure 1 gives the schematic projection of the atoms on the (100) plane. This projection corresponds to the idealized formula*:



without zeolitic water. In this case, the reliability factor:

$$R = \frac{\sum |F_{obs.}| - |F_{calc.}|}{\sum |F_{calc.}|}$$

is $R = 0.42$ for the OkI reflections and $R = 0.29$ for the hOl reflections. Table 1 gives the values of $|F_{hkl}|_{obs.}$ normalized on the $|F_{hkl}|_{calc.}$ based on the model of Brauner and Preisinger.

In this work the R values are large because these factors correspond to a partial summation of $|F_{hkl}|$. Under these conditions a good structural agreement is possible for R values near to 0.20 (Pinsker, 1968).

THE FOURIER ANALYSIS RESULTS

Fourier projections on (100) and (010) planes of all the atoms of the cell and difference projections corresponding to certain atoms only lead to the following observations:

(a) The displacement between tetrahedral sheets is $c/3$ (see Fig. 5 — and ----). The reduction of the relative slip between the tetrahedral sheets in the model is $z/c = 0.017$.

(b) An atom appears in the position $y/b = 0.250$, $z/c = 0.750$ which is unoccupied in the model of Brauner and Preisinger. Study of the partial Fourier projection on the planes (100) and (010) shows that there is in reality a statistical distribution between two sites "4c" (0, $\bar{y}/b, 3/4$) of the magnesium on the edges of the sheets (these sites are marked by $4c_{IV}$

Table 1. Observed and calculated OkI and hOl structure factors for the Brauner and Preisinger model (without zeolitic water)

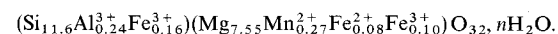
<i>h</i>	<i>k</i>	<i>l</i>	F_{hkl}^{calc}	$ F_{hkl} _{obs}$	<i>h</i>	<i>k</i>	<i>l</i>	F_{hkl}^{calc}	$ F_{hkl} _{obs}$
0	0	0	376.9	377.	0	21	3	-19.2	21.
0	2	0	-1.2	17.	0	23	3	5.9	5.
0	4	0	2.6	20.	0	0	4	21.1	28.
0	6	0	69.5	68.	0	2	4	-4.7	14.
0	8	0	-0.2	16.	0	4	4	4.6	14.
0	10	0	0.0	10.	0	6	4	-4.4	16.
0	12	0	20.8	26.	0	8	4	4.2	12.
0	14	0	-0.4	7.	0	10	4	-3.9	7.
0	16	0	-3.3	21.	0	12	4	3.5	19.
0	18	0	-74.3	68.	0	14	4	-3.1	5.
0	20	0	5.8	12.	0	16	4	2.4	4.
0	22	0	-2.4	10.	0	18	4	-14.7	15.
0	24	0	15.0	22.	0	20	4	3.5	0.
0	1	1	4.6	20.	0	22	4	-2.8	0.
0	3	1	23.4	42.	0	24	4	2.5	5.
0	5	1	2.8	20.	0	1	5	-0.7	8.
0	7	1	-2.3	9.	0	3	5	15.9	17.
0	9	1	3.3	27.	0	5	5	-1.1	5.
0	11	1	-1.7	10.	0	7	5	1.3	10.
0	13	1	1.9	7.	0	9	5	15.4	18.
0	15	1	11.0	24.	2	0	0	-64.5	87.
0	17	1	0.4	4.	4	0	0	107.9	123.
0	19	1	-1.0	5.	6	0	0	-69.8	28.
0	21	1	-7.6	25.	8	0	0	13.9	22.
0	23	1	0.1	5.	10	0	0	31.8	21.
0	0	2	45.7	37.	12	0	0	34.5	14.
0	2	2	-11.8	14.	1	0	2	-48.2	79.
0	4	2	11.1	13.	2	0	2	-34.6	49.
0	6	2	-25.1	24.	3	0	2	-13.7	34.
0	8	2	10.4	9.	4	0	2	-37.6	33.
0	10	2	-9.8	9.	5	0	2	-11.1	20.
0	12	2	-14.9	29.	6	0	2	-44.0	25.
0	14	2	-5.1	8.	7	0	2	-2.1	16.
0	16	2	3.2	11.	8	0	2	-45.7	20.
0	18	2	-47.7	30.	9	0	2	36.4	27.
0	20	2	8.3	7.	10	0	2	16.9	10.
0	22	2	-7.0	4.	11	0	2	-11.4	11.
0	24	2	-6.4	14.	12	0	2	-10.0	12.
0	1	3	-6.5	5.	13	0	2	7.7	13.
0	3	3	36.5	45.	1	0	4	-66.5	46.
0	5	3	-7.5	8.	2	0	4	17.5	23.
0	7	3	8.3	16.	3	0	4	20.0	16.
0	9	3	64.2	68.	4	0	4	10.7	10.
0	11	3	2.3	13.	5	0	4	-40.1	27.
0	13	3	-2.4	8.	6	0	4	7.3	16.
0	15	3	23.2	29.	7	0	4	24.9	17.
0	17	3	-4.5	4.	8	0	4	8.9	12.
0	19	3	3.2	5.	9	0	4	13.1	10.

and $4c_V$ on the Fig. 5). This figure gives the final projection on the (100) plane of the atoms of a quarter of the sepiolite cell. Only the site $4c_{IV}$ with coordinates $x/a = 0.000$, $y/b = 0.196$, $z/c = 0.750$ is occupied by the magnesium on the edges of the sheets in the model of Brauner and Preisinger.

(c) Correlative to the statistical distribution of the magnesium between two sites, the water molecules $H_2O_{cryst.}$ and the hydroxyls also are distributed between two positions:

Approximately a third of the water molecules $H_2O_{cryst.}$ (noted $(H_2O)_1$ in Fig. 7) occupy the position indicated by Brauner and Preisinger ($x/a = 0.083$, $y/b = 0.250$, $z/c = 0.500$) whereas two thirds of these molecules (noted $(H_2O)_2$ in Fig. 7) are on the site whose coordinates are $x/a = 0.130$, $y/b = 0.250$, $z/c = 0.500$. In this new position, the water molecules are nearer the oxygens of the base of the tetrahedral sheet. Hydroxyls also are divided in the same proportion between the Brauner and Preisinger position ($x/a = 0.084$, $y/b = 0.084$, $z/c = 0.079$) and a position noted $(OH)_2$ in Fig. 6 whose coordinates are ($x/a = 0.084$, $y/b = 0.104$, $z/c = 0.119$). This displacement may be explained by a local distortion of the crystalline field when the $4c_V$ position is occupied by magnesium.

* The chemical analysis of the Ampandrandava sepiolite (Madagascar), was made by Caillère (1972) and gives the structural formula:



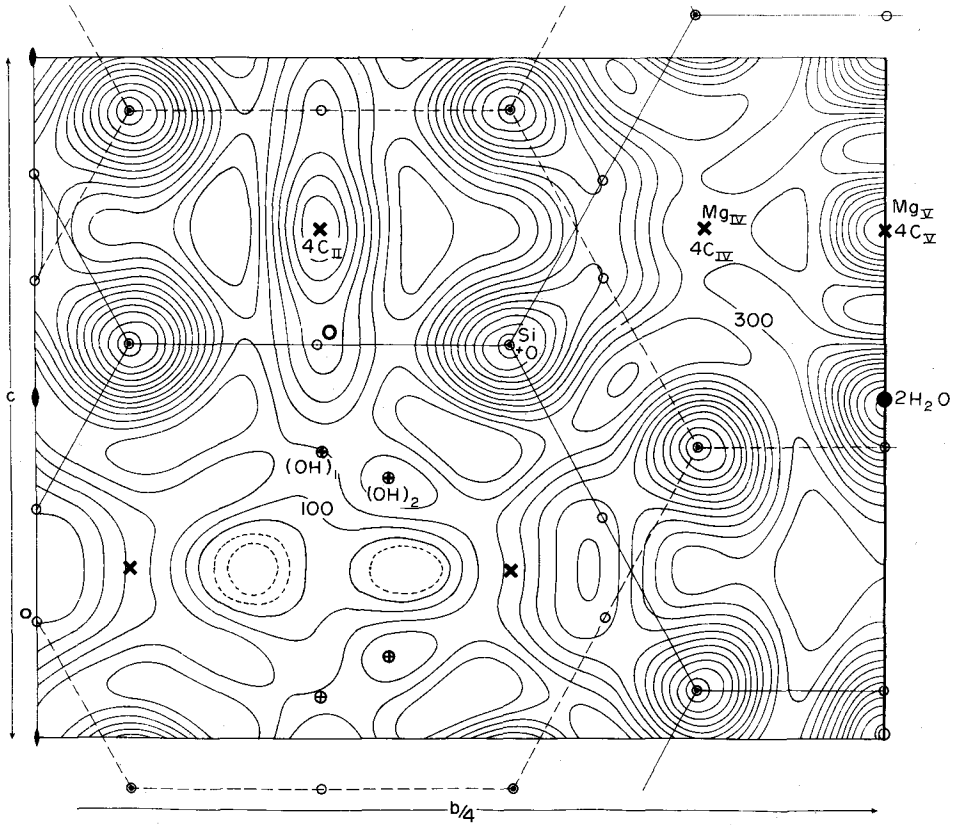


Fig. 5. Fourier projection on (100) plane of 1/4 of sepiolite unit cell.

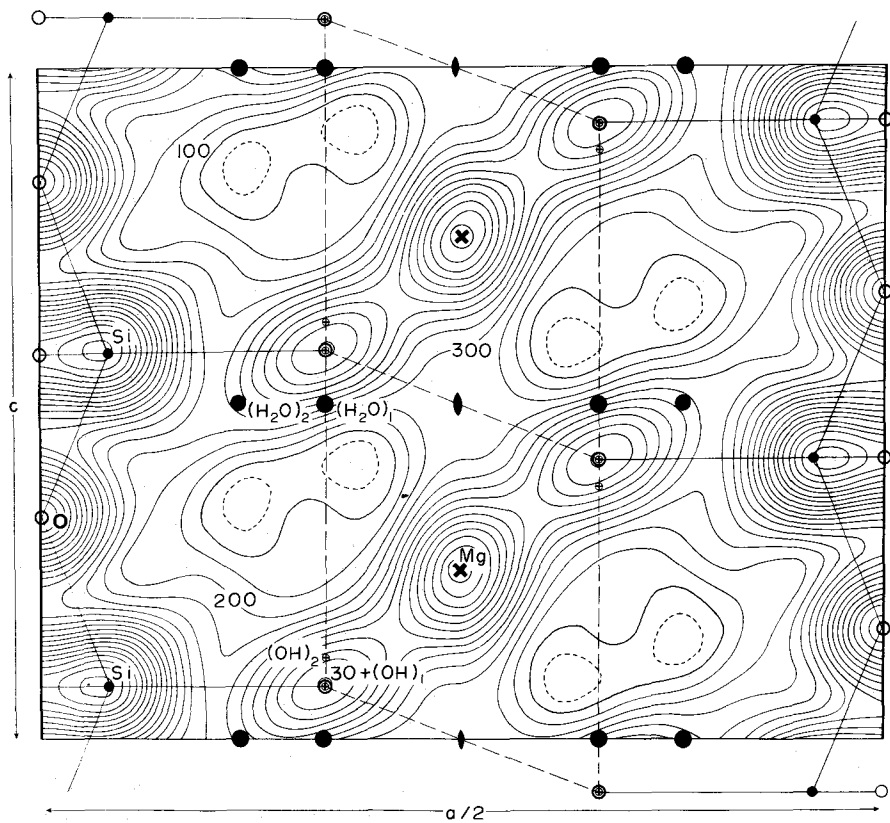


Fig. 6. Fourier projection on (010) plane of 1/2 of sepiolite unit cell.

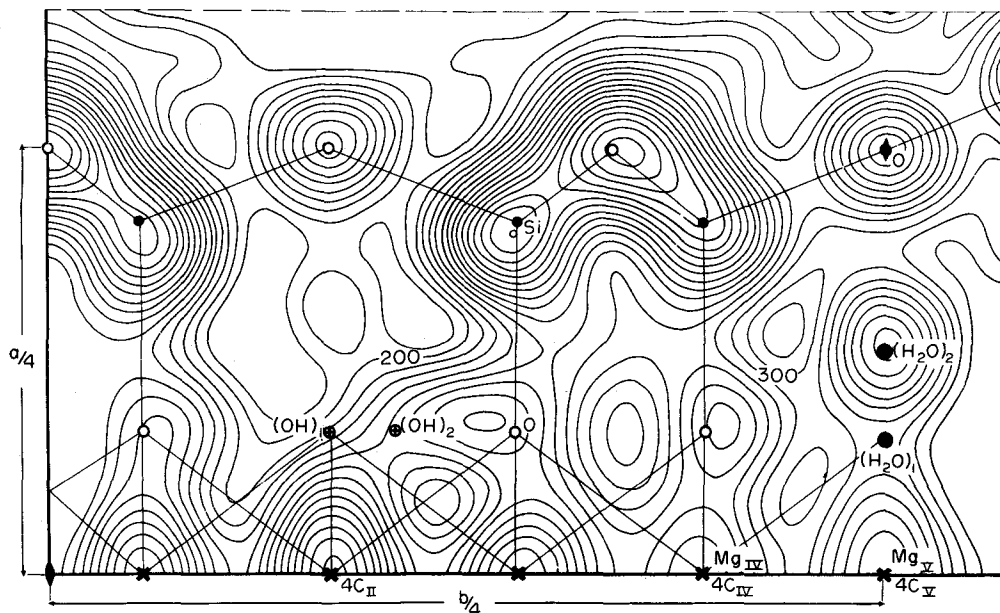


Fig. 7. Fourier projection on (001) plane of 1/16 of sepiolite unit cell.

(d) Finally, partial Fourier projection seems to indicate that isomorphous substitutions in the octahedral sheet are preferentially in site $4c_{II}$ ($x/a = 0.000$, $y/b = 0.084$, $z/c = 0.750$).

In all the experimental projections, the maximum of this position is higher than the maximum of the other octahedral positions.

The Fourier projections shown in Fig. 5 and 6 are those obtained for the model presently described. Full

Table 2. Atomic coordinates for the proposed model of sepiolite

Atom	Fraction	x/a	y/b	z/c	equivalent positions
Mg I	1.00	0.000	0.028	0.250	4
MgII	0.77	0.000	0.084	0.750	4
MnII	0.14	0.000	0.084	0.750	
FeII	0.09	0.000	0.084	0.750	
MgIII	1.00	0.000	0.140	0.250	4
MgIV	0.33	0.000	0.196	0.750	4
MgV	0.67	0.000	0.250	0.750	
Si I	0.97	0.208	0.028	0.579	8
Al I	0.02	0.208	0.028	0.579	
Fe I	0.01	0.208	0.028	0.579	
Si II	0.97	0.208	0.140	0.579	8
Al II	0.02	0.208	0.140	0.579	
Fe II	0.01	0.208	0.140	0.579	
Si III	0.97	0.208	0.196	0.079	8
Al III	0.02	0.208	0.196	0.079	
Fe III	0.01	0.208	0.196	0.079	
O I	1.00	0.084	0.028	0.579	8
O II	1.00	0.084	0.140	0.579	8
O III	1.00	0.084	0.196	0.079	8
O IV	1.00	0.250	0.000	0.329	8
O V	1.00	0.250	0.084	0.579	8
O VI	1.00	0.250	0.168	0.329	8
O VII	1.00	0.250	0.168	0.829	8
O VIII	1.00	0.250	0.250	0.079	4
(OH) ₁	0.33	0.084	0.084	0.079	8
(OH) ₂	0.67	0.084	0.104	0.119	
(H ₂ O _{cryst.}) ₁	0.33	0.084	0.250	0.500	8
(H ₂ O _{cryst.}) ₂	0.67	0.130	0.250	0.500	

lines represent equipotential curves, with a step of 100 arbitrary units between each line, and the dotted lines are for the negative portions. Figure 5 gives the Fourier projection on the plane of the atoms of a quarter of the sepiolite cell (this projection has a mirror image at $y/b = 0.250$). Figure 6 gives the projection on the plane (010) for half a cell of sepiolite (this projection has a mirror at $x/a = 0.250$). This last projection shows a complete element of the layer. For our model the reliability factor is $R = 0.23$ for the reflections $Ok1$ and $R = 0.24$ for the reflections hOl .

Finally, the Fourier projection on the plane (001) is presented by means of the hkO reflections. Because the intensities are perturbed by dynamic interactions, this projection was not employed in the determination of atomic coordinates. Nevertheless Fig. 7 shows clearly the distribution between two sites of the magnesium at the edges of the sheets. It also clearly shows the new position of some water molecules (noted $(H_2O)_2$ on Fig. 7). Table 2 gives the atomic coordinates of the proposed model. Table 3 gives the observed and calculated $Ok1$ and hOl structure factors for the final model.

RELATIONSHIP BETWEEN THE PHYSICO-CHEMICAL PROPERTIES OF SEPIOLITE AND THE STRUCTURAL FEATURES

The previously known models of sepiolite do not give a satisfactory interpretation of water desorption and of the fixation of polar molecules. Indeed, previous studies (Caillère, 1936; Martin-Vivaldi and Cano-Ruiz, 1955; Prost, 1973; Serna, 1973; Nagata *et al.*, 1974) on the dehydration of sepiolite have shown two weight losses of bound water between 250 and 650°C at normal pressure. Figure 8 shows the

Table 3. Observed and calculated *Okl* and *hOl* structure factors for the final model

<i>h</i>	<i>k</i>	<i>l</i>	F_{hkl}^{calc}	$ F_{hkl}^{obs} $	<i>h</i>	<i>k</i>	<i>l</i>	F_{hkl}^{calc}	$ F_{hkl}^{obs} $
0	0	0	379.7	380.	0	23	3	5.6	4.
0	2	0	-5.5	15.	0	0	4	-13.2	24.
0	4	0	6.8	18.	0	2	4	-6.1	12.
0	6	0	57.6	61.	0	4	4	9.6	12.
0	8	0	21.0	15.	0	6	4	-17.2	14.
0	10	0	-6.9	9.	0	8	4	6.9	10.
0	12	0	22.4	23.	0	10	4	-11.9	6.
0	14	0	-12.4	7.	0	12	4	5.1	16.
0	16	0	-2.6	19.	0	14	4	-2.1	4.
0	18	0	-67.2	61.	0	16	4	5.1	4.
0	20	0	11.5	11.	0	18	4	-7.1	13.
0	22	0	-6.5	9.	0	20	4	0.7	0.
0	24	0	11.4	19.	0	22	4	-2.9	0.
0	1	1	3.7	18.	0	24	4	5.1	4.
0	3	1	27.0	37.	0	1	5	2.5	7.
0	5	1	14.4	17.	0	3	5	13.3	15.
0	7	1	-9.9	8.	0	5	5	2.8	4.
0	9	1	20.0	24.	0	7	5	-5.8	8.
0	11	1	-15.8	9.	0	9	5	7.3	16.
0	13	1	5.6	6.	2	0	0	-69.2	84.
0	15	1	17.5	21.	4	0	0	106.1	119.
0	17	1	5.2	4.	6	0	0	-62.9	27.
0	19	1	-2.1	4.	8	0	0	27.3	21.
0	21	1	-14.5	22.	10	0	0	24.2	20.
0	23	1	-3.8	4.	12	0	0	34.1	13.
0	0	2	25.4	33.	1	0	2	-57.8	76.
0	2	2	-14.0	12.	2	0	2	-39.7	47.
0	4	2	10.3	11.	3	0	2	-17.6	32.
0	6	2	-10.9	21.	4	0	2	-39.1	32.
0	8	2	5.6	8.	5	0	2	-12.9	19.
0	10	2	-5.0	8.	6	0	2	-31.4	24.
0	12	2	-18.5	25.	7	0	2	-3.4	15.
0	14	2	-5.6	7.	8	0	2	-33.8	19.
0	16	2	5.6	10.	9	0	2	45.6	26.
0	18	2	-31.7	27.	10	0	2	7.0	10.
0	20	2	9.0	6.	11	0	2	-15.3	11.
0	22	2	-7.0	3.	12	0	2	-18.6	11.
0	24	2	-8.6	12.	13	0	2	11.2	12.
0	1	3	-7.5	5.	1	0	4	-59.4	44.
0	3	3	41.3	40.	2	0	4	30.3	22.
0	5	3	-8.8	7.	3	0	4	22.0	16.
0	7	3	15.9	14.	4	0	4	0.2	10.
0	9	3	59.9	61.	5	0	4	-36.4	26.
0	11	3	2.7	11.	6	0	4	32.0	16.
0	13	3	-6.6	7.	7	0	4	23.1	17.
0	15	3	30.8	26.	8	0	4	14.0	12.
0	17	3	-0.9	3.	9	0	4	7.5	10.
0	19	3	2.3	4.					
0	21	3	-25.8	19.					

thermogravimetric analysis obtained for three samples from Ampandrandava, Vallecas and Salinelles. All samples heated to 150°C have an initial weight loss of 12–15% which corresponds to zeolitic

water. The weight loss between 250°C and 650°C is between 4 and 6% and corresponds to the removal of water bound to magnesium on the edges of the sheets. Above 650°C a total loss of 3% corresponds to dehydroxylation of the mineral. The total loss is in accordance with the Brauner and Preisinger model. However there are clearly two stages of loss between 250 and 650°C. The first from 250 to 400°C and the second from 400 to 650°C. These two stages are also present in the dehydration curves of sepiolite in vacuum around to 10⁻⁵ Torr (curve 4 on Fig. 8). These results cannot be interpreted by the Brauner and Preisinger model which has only one type of bound water.

Examination of the i.r. absorption spectrum of sepiolite heated to 300°C under vacuum shows a doublet at 1616–1624 cm⁻¹ corresponding to the bending vibrations. On heating sepiolite above 400°C, only the band at 1616 cm⁻¹ remains (see Fig. 9). Other studies by i.r. spectroscopy (Prost, 1973; Serna, 1973; Serna *et al.*, 1974) are in good agreement with their model and particularly with the distinction of two types of bound water, which appear as a doublet at both 1616–1624 cm⁻¹ (bending vibration) and at 3560–3620 cm⁻¹ (stretching vibration). Only the band at 1624 cm⁻¹ disappears on dehydration of the mineral at the second stage of thermogravimetric analysis. The 1624 cm⁻¹ vibration thus corresponds to the less tightly bound water. Infrared spectroscopic studies on the absorption of polar molecules (Serna, 1973; Serna *et al.*, 1974) indicate that methanol will replace the less tightly bound water whereas acetone becomes attached to these water molecules. After acetone fixation on the accessible water, the absorption band at 1624 cm⁻¹ shifts to 1654 cm⁻¹. However this band disappears completely when water is replaced by methanol. In these two cases the band at 1616 cm⁻¹ is unaltered.

All of these results confirm the existence of the two

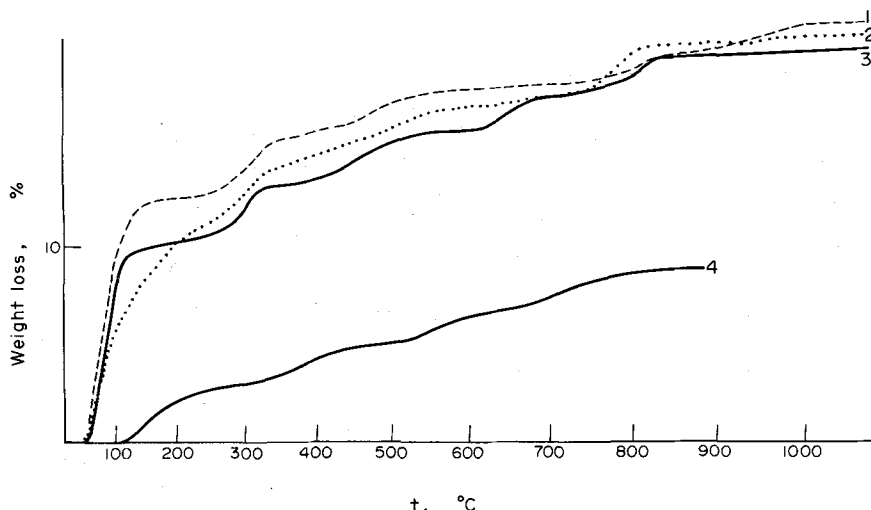


Fig. 8. Thermogravimetric analysis of sepiolite of Salinelles (curve 1), Ampandrandava (curve 2) and Vallecas (curve 3) at normal pressure. Curve 4 shows thermogravimetric analysis of Vallecas sepiolite in vacuum (10⁻⁵ Torr).

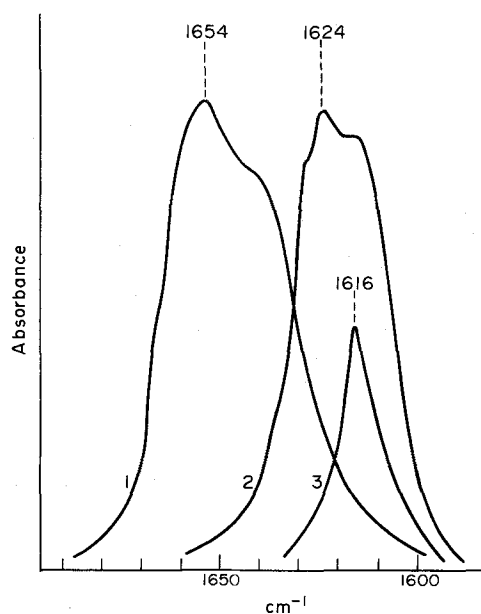


Fig. 9. OH bending vibration of bound water: 1—normal conditions, 2—vacuum (10^{-5} Torr), 3— 300°C in vacuum (Perkin-Elmer 1800 I.R. spectrocope).

following types of bound water molecules: water molecules bound to the magnesium in the position designated by the model of Brauner and Preisinger; water molecules bound to the magnesium in a pre-determined position and which corresponds to a displacement of these atoms in the channels.

With this structural model it can be concluded that the bound water in the more asymmetric octahedral sites is rather reactive and mobile. This explains the persistence of the band at 1614 cm^{-1} when heated to 300°C and in the case of adsorption of methanol and acetone. This band corresponds to the fraction of bound water which has the higher bonding energy and the lower reactivity.

CONCLUSIONS

Structure analysis of sepiolite with electron diffraction data shows that the principal differences between the proposed model and the Brauner and Preisinger model are two positions for the magnesium on the edges of the sheets and two positions of associated water molecules.

Brauner and Preisinger studied sepiolite under "normal" humidity conditions, with zeolitic water in the channels. Under these conditions it is not excluded that all the Mg^{2+} cations of the edges of the sheets occupy the very symmetrical octahedral sites. By elimination of zeolitic water in vacuum (as it is the case in electron diffraction), part of these Mg^{2+} cations are displaced from the edges of the sheets by a partial hydrolysis. In this hypothesis, under normal conditions the structure of sepiolite is near that of Brauner and Preisinger. On the other hand this model should be taken as a basis for studying sepiolite in vacuum, especially for adsorption of organic molecules.

Acknowledgement—We are obliged to Professor J. M. Serratos and Dr. C. Serna for their collaboration in making the i.r. studies of these sepiolites. Professor S. Caillère supplied the chemical analysis. M. Seto translated the original text. We wish to thank them for their valuable assistance.

REFERENCES

- Allpress, J. G. and Sanders, J. V. (1973) The direct observation of the structures of real crystals by lattice imaging. *J. appl. Crystallogr.* **6**, 165–190.
- Brauner, L. and Preisinger, A. (1956) Struktur und entstehung des sepioliths. *Tschermaks Min. Petr. Mitt.* **6**, 120–140.
- Brindley, G. W. (1959) X-Ray and electron diffraction data for sepiolite. *Am. Miner.* **44**, 495–500.
- Caillère, S. (1936) Thermal studies. *Bull. Soc. Franc. Miner.* **59**, 353–374.
- Cowley, J. M. and Moodie, A. F. (1962) The scattering of electrons by thin crystals. *J. Phys. Soc. Japan.* **17**, 86–91.
- Cowley, J. M. (1968) Acta geologica et geographica Universitatis Comenianae. No. 14. Slovenské Pedagogické Nakladatelstvo, Bratislava.
- Martin-Vivaldi, J. L. and Cano-Ruiz, J. (1955) Contribution to the study of sepiolite: some consideration regarding the mineralogical formula. *Clays and Clay Minerals, 4th Nat. Conf. U.S., N.R.C.*, 1956. 173–176.
- Martin-Vivaldi, J. L. and Robertson, R. H. S. (1971) *The Electron Optical Investigation of Clays* (Edited by J. A. Gard), pp. 255–275. London Mineralogical Society.
- Menter, J. W. (1956) Electron microscopy. *Proc. Stockholm Conf.* (Edited by Almqvist and Wiksel) pp. 88–93.
- Nagata Hiroshi, Susumu Shimoda and Toshio Sudo (1974) On dehydration of bound water of sepiolite. *Clays and Clay Minerals* **22**, 285–293.
- Nagy, B. and Bradley, W. F. (1955) The structural scheme of sepiolite. *Am. Miner.* **40**, 885–892.
- Pinsker, Z. G. (1968) Physical principles and certain results of the modern electron diffraction structure analysis. Acta geologica et geographica Universitatis Comenianae 14. Slovenské pedagogické nakladatelstvo, Bratislava.
- Preisinger, A. (1963) Sepiolite and related compounds: its stability and application. *Clays and Clay Minerals, Proc. Nat. Conf.*, Vol. 10, pp. 365–371. Pergamon Press, Oxford.
- Prost, R. (1973) Spectre infra-rouge de l'eau présente dans l'attapulgite et dans la sépiolite. *Bull. Gr. Franç. Argiles.* **25**, 53–63.
- Rautureau, M. and Tchoubar, C. (1972) Etude morphologique de la sépiolite par microscopie électronique. *J. Microsc.* **14**, 139–146.
- Rautureau, M., Tchoubar, C. and Mering, J. (1972) Analyse structurale de la sépiolite par microdiffraction électronique. *C. r. Acad. Sci.* **274**, 269–271.
- Rautureau, M., Tchoubar, C. and Mering, J. (1972) Analyse structurale de la sépiolite à partir des données de la diffraction électronique. *Int. Clay Conf. Madrid* (Edited by J. M. Serratos) pp. 115–121.
- Serna, J. C. (1973) Naturaleza y propiedades de la superficie de la sepiolita. Thesis, University of Madrid.
- Serna, J. C., Rautureau, M., Prost, R., Tchoubar, C. and Serratos, J. M. (1974) Etude de la sépiolite à l'aide des données de la microscopie électronique, de l'analyse thermopondérale et de la spectroscopie infra-rouge. *Bull. Groupe Franç. Argiles* **26**, 153–163.
- Tchoubar, C., Rautureau, M., Clinard, C. and Ragot, J. P. (1973) Technique d'inclusion appliquée à l'étude des silicates lamellaires et fibreux. *J. Microsc.* **18**, 147–154.
- Zvyagin, B. B. (1967) *Electron Diffraction Analysis of Clay Mineral Structures*. Plenum Press, New York.